Supplementary online material

Direct ageing experiments on nanometre-scale aluminium alloy samples

J. Banhart[1*,2], Y.-S. Chen[1], Q.N. Guo[2], R.K.W. Marceau[3], J.M. Cairney[1]

[1] Australian Centre for Microscopy and Microanalysis, The University of Sydney, NSW 2006, Australia

[2] Helmholtz Zentrum Berlin for Materials and Energy, Hahn-Meitner-Platz 1, 14109 Berlin, Germany

[3] Deakin University, Institute for Frontier Materials, Geelong, Victoria 3216, Australia

* temporary affiliation

S1. Vapour pressure of elements

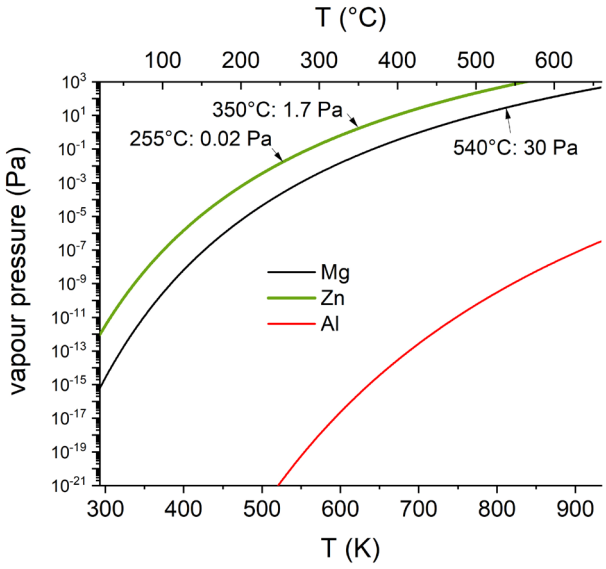

Fig. S1. Vapour pressures of Al, Mg and Zn calculated using the parametrisation $\log\left(\frac{p}{\mathrm{atm}}\right) = A + BT + C\log(T)$ and tabulated coefficients A, B, C [1]. For Zn, values for both the highest and lowest solutionising temperature applied in this work are given. A value for Mg at the solutionising temperature of the Al-Mg-Si alloy is also specified.

The vapour pressure of a component of an alloy determines how fast this component is depleted during solutionising. Mg and Zn are known to have high vapour pressures and therefore attention has to be paid to possible losses. In bulk alloys, losses are limited to areas close to the surface and bulk compositions measured after solutionising do not show notable composition changes. Depletion of Mg from Al-Mg-Si alloys has been investigated by various researchers ([2, 3] and others) mostly by measuring global properties. Concentration profiling led to the conclusion that Mg depletion during solutionising in air is limited to a 10-µm thick surface layer [4], which implies that age hardening of most engineering parts will hardly be affected. In the present work, however, the situation is different since atom probe samples of very small

dimensions are solutionised. Therefore losses have to be expected and the selection of suitable solutionising temperatures and times is important.

S2. Atom probe mass spectra

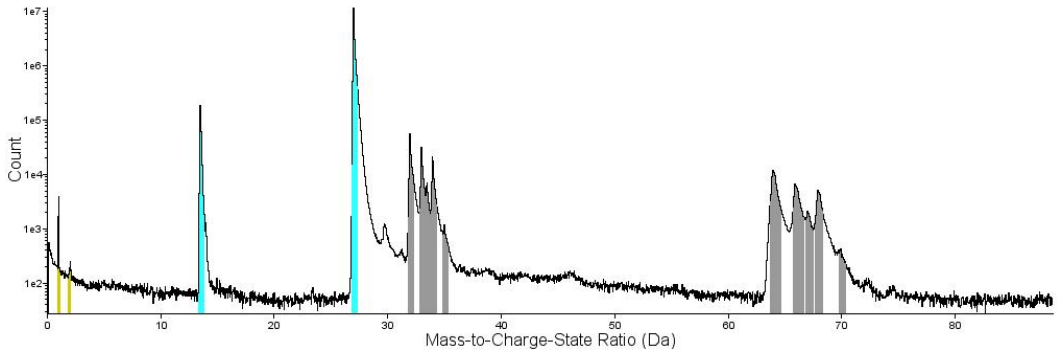

Fig. S2. Typical mass spectrum of Al-Zn alloy obtained by APT. Hydrogen (dark yellow, 2 isotopes), Al (cyan, single and double charge, 1 isotope) and Zn (grey, single and double charge, 5 isotopes) are detected.

The mass spectra obtained can be easily decomposed into Al and Zn contributions.

S3. Calculation of radial distribution functions

Program IVAS 3.6 provides a built-in function for calculating radial distribution functions but this has not been used here because some subtleties of averaging have to be considered and it is not entirely clear how IVAS handles these.

Radial distribution functions are obtained by considering concentric spheres of radius R of spacing ΔR around a given central Zn atom (indexed by i) in an APT data set, counting the number of Zn atoms in each shell between two adjacent spheres,

$$N_{\mathrm{Zn,i}}(R, \Delta R), \tag{1}$$

and then averaging these histograms over all n_{Zn} central Zn atoms selected:

$$\bar{N}_{\mathrm{Zn}}(R, \Delta R) = \sum_{i=1}^{n_{\mathrm{Zn}}} \frac{N_{\mathrm{Zn,i}}(R,\Delta R)}{n_{\mathrm{Zn}}}. \tag{2}$$

Evaluation of Eq. (2) can be time consuming for large data sets because many distances between pairs of Zn atoms have to be calculated.

A completely random distribution of Zn atoms should yield a constant value for $N_{\mathrm{Zn}}(R, \Delta R)$ if normalised by the volume of the respective shell and clustering would be detected by an increased value for small R. However, due to non-uniform atomic densities in APT data sets it is preferable to eliminate such effects by comparing $\bar{N}_{\mathrm{Zn}}(R, \Delta R)$ to the analogous quantity calculated for a randomised data set in which all atomic coordinates are kept constant but the atomic types are reshuffled randomly, leading to

$$N_{\mathrm{Zn},i}^{\mathrm{rnd}}(R, \Delta R) \tag{3}$$

instead of Eq. (1). This quantity is also averaged over all selected central Zn atoms i, yielding the analogy to Eq. (2). We then consider the ratio

$$f_{\mathrm{Zn}}(R, \Delta R) = \frac{\bar{N}_{\mathrm{Zn}}(R, \Delta R)}{\bar{N}_{\mathrm{Zn}}^{\mathrm{rnd}}(R, \Delta R)}, \tag{4}$$

which should be close to unity for a random distribution of Zn atoms. The randomisation process can be carried out in various ways. Most simply one could give all Zn atoms a new position simultaneously and then calculate $\bar{N}_{\mathrm{Zn}}^{\mathrm{rnd}}(R, \Delta R)$ based on the resulting random distribution. Because the number of Zn atoms has to be kept constant, Zn atoms will move to positions occupied by Al in the APT data set, which implies that the positions of the central Zn atoms in the nominator and the denominator of Eq. (4) are no longer the same, which possibly has a small influence on the result. To avoid this, one can fix the position of just one central Zn atom and randomly reallocate the remaining $(n_{\mathrm{Zn}} - 1)$ Zn atoms (also implying moving Zn to Al positions) and calculate Eq. (3). This has to be done n_{Zn} times before calculating an average analogous to Eq. (2). Now, the averages $\bar{N}_{\mathrm{Zn}}(R, \Delta R)$ and $\bar{N}_{\mathrm{Zn},i}^{\mathrm{rnd}}(R, \Delta R)$ are based on the same central Zn atom positions but a lot of computation time is consumed if n_{Zn} represents many thousands of atoms. Therefore, we choose the compromise to fix the position of a subset $\{\mathrm{Zn}\}_k$ of 1% of all Zn atoms and to randomise the remaining 99%. This is repeated $K = 100$ times for disjunct subsets, after which an average of the 100 resulting $N_{\{\mathrm{Zn}\}_k}^{\mathrm{rnd}}$ is computed.

Another aspect is that of statistical fluctuations. For small R, $N_{\mathrm{Zn,i}}$ in Eq. (1) can be as small as 100. Randomisation then leads to fluctuations of the order $\sqrt{N_{\mathrm{Zn},i}^{\mathrm{rnd}}}$ in the denominator of Eq. (4), i.e. up to 10% of the entire expression. As we wish to discuss minute deviations of Eq. (4) from unity in this paper, a reduction of such fluctuations is sought by repeating the calculation of $\bar{N}_{\mathrm{Zn}}^{\mathrm{rnd}}$ J times (we choose J = 100) with different randomisations and averaging the results. This should bring down fluctuations to 1%. Eventually, the denominator in Eq. (4) turns into

$$\bar{N}_{\mathrm{Zn}}^{\mathrm{rnd}}(R,\Delta R)=\frac{1}{KJ}\sum_{j=1}^{J}\underbrace{\sum_{k=1}^{K}N_{\{Zn\}_k}^{\mathrm{rnd,j}}(R,\Delta R)}_{\bar{N}_{\mathrm{Zn}}^{\mathrm{rnd,j}}}. \tag{6}$$

The value for f calculated from Eq. (4) will still deviate from 1 even for perfectly random Zn contributions. For the denominator, we use the standard deviation of the J different randomisations $N_{\mathrm{Zn}}^{\mathrm{rnd,j}}$ from their average value $\bar{N}_{\mathrm{Zn}}^{\mathrm{rnd}}$ as an uncertainty ΔN^{rnd} and write for the uncertainty of f (dropping the index Zn and the argument $(R,\Delta R)$):

$$\Delta f = N\frac{\Delta N^{\mathrm{rnd}}}{\left(N^{\mathrm{rnd}}\right)^2}=f\frac{\Delta N^{\mathrm{rnd}}}{\bar{N}^{\mathrm{rnd}}},\quad \text{with}\quad \Delta N^{\mathrm{rnd}}=\sqrt{\frac{\sum_{j=1}^{J}\left(N_{\mathrm{Zn}}^{\mathrm{rnd,j}}-\bar{N}_{\mathrm{Zn}}^{\mathrm{rnd}}\right)^2}{J}}. \tag{7}$$

Another choice to be made is that of the central Zn atoms to be included in Eq. (2). We calculate $N_{\mathrm{Zn,i}}(R,\Delta R)$ and $N_{\mathrm{Zn}}^{\mathrm{rnd}}(R,\Delta R)$ for Zn atoms within a sphere of radius R_1 =10 nm around a given origin in the APT data (yellow spheres in Fig. S3) and let R range up to R = 10 nm. This implies that Zn atoms within a sphere of radius R_2 =20 nm around the origin contribute to Eqs. (1) and (3) (e.g. dashed orange sphere). We make sure that the entire sphere of radius R_2 lies inside the APT data set. When randomising the Zn distribution, the Zn concentration within the central sphere and the outer region (orange sphere without the yellow sphere) are kept constant separately so that the number of Zn atoms in the inner sphere is the same in all randomised data sets. Depending on how big the APT data set is, various points of origin are chosen for independent calculations that are then averaged (9 in the example shown in Fig. S3).

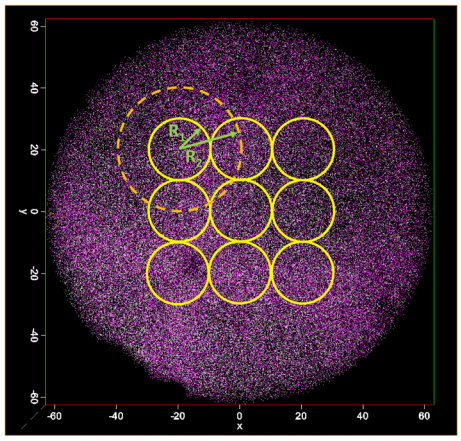

Figure S3. Definition of averaging volumes in the (x,y) plane of an APT data set (units are nm). The broken and solid circles defines concentric spheres of radius $R_2 = 2R_1$ = 20 nm. The inner volume (yellow) contains all the central Zn atoms that are included in Eqs. (1) and (3), the outer volume (orange, shown for just one sphere) all the Zn atoms that are at 10 nm distance from any atom in the inner (yellow) sphere.

With all these measures we minimise effects on $f_{\mathrm{Zn}}(R, \Delta R)$ not caused by clustering but by density fluctuations in the APT data set and other distortions. Test calculations of various data sets, where both Al and Zn positions were randomised without constraints show that $f_{\mathrm{Zn}}(R, \Delta R)$ is equal to 1 within a margin of 0.01 for small R and 0.003 for larger values up to 10 nm, see Fig. S4.

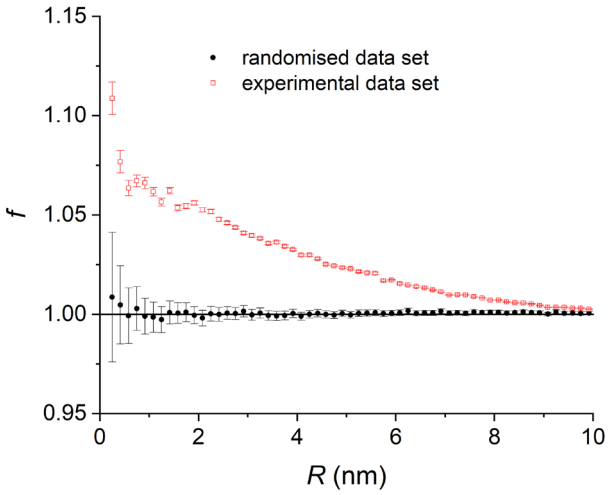

Fig. S4. $f_{\mathrm{Zn}}(R, \Delta R)$ of the data set shown in Fig. 4 of the main paper (red open symbols) but with a randomisation of all the Al and Zn atom positions (black full symbols).

The procedure described here for calculating RDFs is inspired by procedures given in Ref. [5]. It differs by the slightly different error calculation and by the details of averaging described above. Moreover, we do use ratios f and not cumulated ratios as in Ref. [5]. Altogether, however, the rationale of the calculation is the same, namely to prove the absence of clustering.

S4. Experiments on Al-Mg-Si alloys

Nano-solutionising experiments were carried out on some APT samples made of Al – 0.6wt% Mg – 0.8 wt.% Si alloy. The samples were crimped inside Inconel tubes instead of Cu as for Al-Zn alloys to avoid the formation of a low-melting Al-Cu eutectic during solutionising. The samples were mounted in a holder of the type shown in Fig. 1 of the main paper and sealed in evacuated Pyrex tubes. Solutionising was performed at 540 °C for effectively 10 min (+ 5 min needed to reach the end temperature), after which the APT samples were cooled in air.

APT experiments were successful and 15 million atoms could be detected in one case. However, the time-of-flight mass spectra showed no trace of Mg unlike in samples that were bulk solutionised, see Fig. S5b, compared to a spectrum obtained on a bulk-solutionised sample that

shows Mg (0.6 at.%), Al and Si (0.7 at.%) in approximately the correct intensities, see Fig. S5a (note that the concentration analysis also includes peaks not shown here). The loss of Mg was expected in view of the very high vapour pressure of Mg, see Fig. S1, which is actually 10 to 100 times higher than that of Zn in Al-Zn alloys at the respective solutionising temperatures. Ref. [5] reports that the Mg content in a similar alloy was notably reduced after ageing thin Al-Mg-Si samples of 20 µm tip radius, from which APT samples were prepared in a second step (see also Ref. [6]). Fig. S5b also shows that the intensity of the Si peaks is greatly reduced (to 0.085 at.%), corresponding to a loss of 90% of the Si atoms, which is unexpected because a very high suspected vapour pressure of Si.

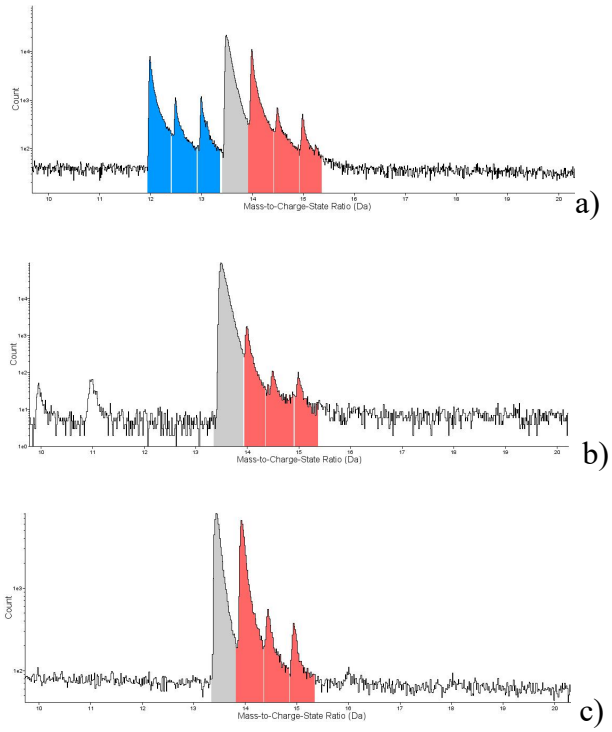

Fig. S5. Range of mass spectra of Al-Mg-Si alloy in which the peaks of doubly charged Al, Mg and Si ions are observed (blue=three isotopes of Mg, grey=one isotope of Al, red= three isotopes of Si). a) bulk-solutionised at 540 °C for 30 min, quenched and NA, b) nano-solutionised at 540 °C for 10 min (excluding heating ramp of about 5 min), quenched and NA. c) sample with a protective Pt cap applied, nano-solutionised at 535 °C for 5 min (excluding heating ramp of about 5 min), quenched and NA.

In an attempt to prevent total loss of Mg, a Pt cap was deposited on two APT samples before solutionising using a Focussed-Ion Beam facility 'Thermofisher G4 Hydra Plasma FIB-SEM', thus providing a protective layer around the tip and part of the shank of the sample. The solutionising temperature was reduced to 535 °C, solutionising time to 5 min (+ 5 min heating

time). After solutionising the cap was removed in the FIB and an APT experiment started. Again, no Mg was detected in the two mass spectra, but the Si peaks show very high intensities (corresponding to 1.8 at.%), i.e. no losses of Si are recorded, see Fig. S5b. As a total of only 4 experiments are available on nano-solutionised samples (2 each for unprotected and Pt-cap-protected APT samples), the phenomenon of varying Si concentration cannot be fully explained at this stage.

In summary, Al-Mg-Si APT samples are very robust considering that they survive solutionising at 540 °C and quenching, but Mg cannot be retained in the samples. Once in-situ flash ageing facilities become available (see comments in Sec. 3.5 of main paper) such experiments could become feasible through a reduction of solutionising times down to seconds.

S5. Radial distribution functions of naturally aged samples

Fig. 6a of the main paper shows the relative radial distribution function of a sample that was first nano-solutionised and quenched and later re-polished to expose deeper lying areas and to have them in the tip area of the APT sample. In order to compare this result to that of samples bulk-solutionised, quenched and aged, Figs. S6 and S7 contain data for two such samples. Obviously, the clusters are much coarser for the sample naturally aged for 8 d (bottom row) than for the sample aged for just 4.5 hours (top row). Quantitative cluster analysis (2nd column) shows this more clearly and also provides some quantitative numbers: the short ageing time give rise to clusters that contain on average 60 atoms, whereas 8 d of ageing creates average cluster sizes of 130 atoms. The largest cluster in the sample aged for 4.5 h contains 1700 atoms, in the sample aged for 8 d 3800 atoms.

The frequency histograms of the nearest neighbour distributions reflect the deviation from a random distribution very clearly and again, the long ageing time gives rise to the biggest deviation.

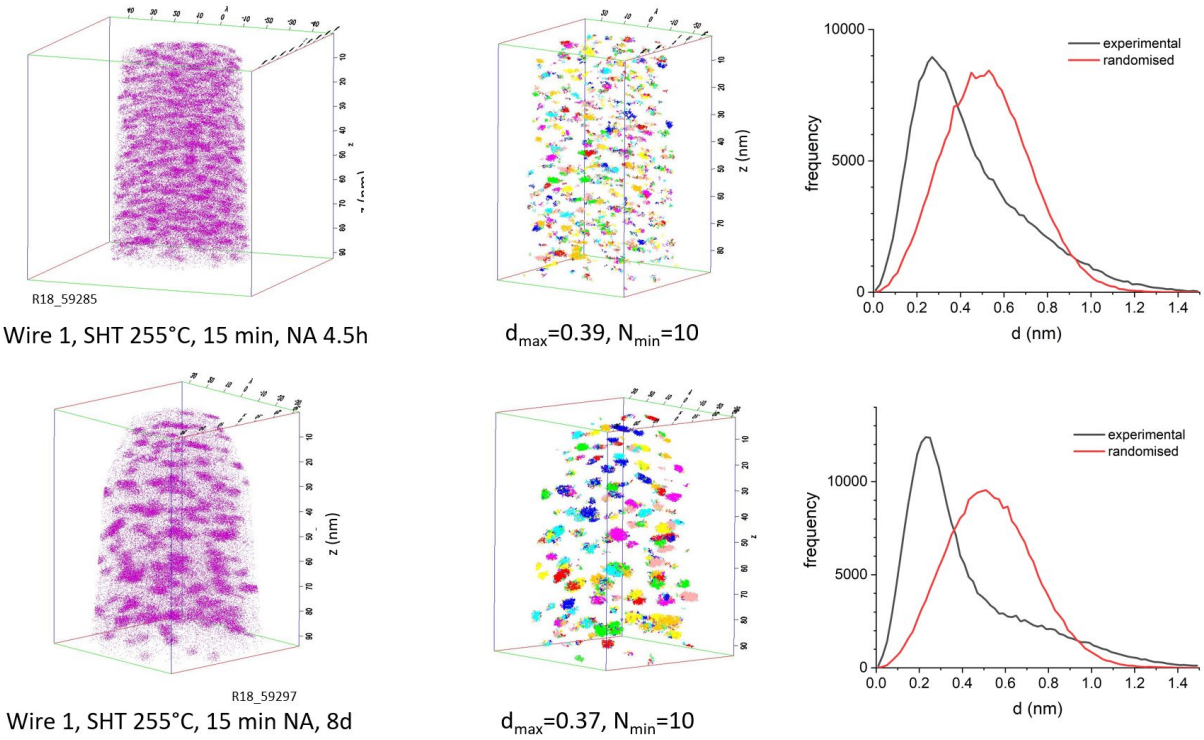

Fig. S6. Bulk solutionised and naturally aged samples Al-Zn samples. Left column: depiction of Zn atoms and specifications of sample and ageing procedures, middle: result of cluster analysis applying the maximum separation algorithm using the specified parameters, right: frequency histograms of 1NN distances.

The radial distribution functions in Fig. S7 all show the profile already noted for the re-polished sample in Fig. 6a of the main paper, namely a high initial value, a decrease to 1 and a zone of values slightly below 1 above a certain radius $R_{\mathrm{RDF=1}}$. This value of the radius roughly corresponds to the observed cluster size. Assuming spherical clusters, the above mentioned numbers of atoms in the largest cluster translates to radii of 2.3 nm and 3 nm, respectively (taking into account a detection efficiency of 57%). As the clusters are not all spherical the clusters are more extended and enhanced Zn-Zn (f>1) correlation exists for larger distances, namely 3.8 nm and 5 nm in Fig. S7. For even larger values of R, f<1 indicates a Zn depletion zone around the clusters. Considering a broad cluster size variation the information contained in f is highly convoluted. Fig. S7 shows clearly that the volumes in re-polished samples are no different from volumes in bulk-aged and NA samples.

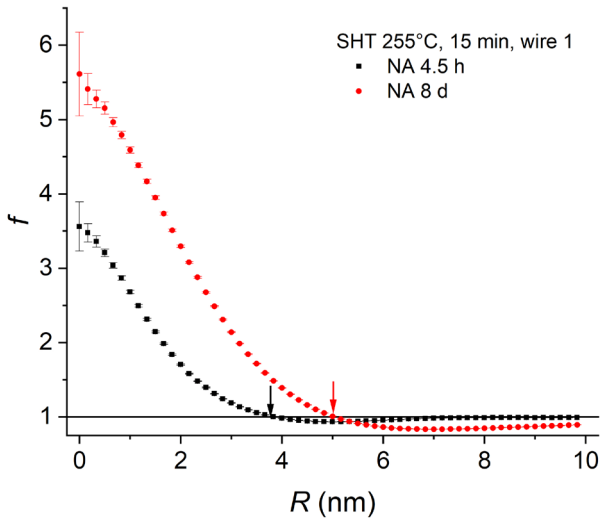

Fig. S7. $f_{\mathrm{Zn}}(R, \Delta R)$ of the data sets shown in Fig. S6. Arrows mark the radius at which $f = 1$.

References

[1] C.B. Alcock, V.P. Itkin, M.K. Horrigan, Vapour pressure equations for the metallic elements: 298–2500K, Can. Metall. Quart. 23 (1984) 309-313.

[2] D.K. Chatterjee, K.M. Entwistle, Study of effect of magnesium loss and of addition of copper on aging of aluminum-magnesium-silicon alloys, J. Inst. Met. London 101 (1973) 53-59.

[3] I. Kovács, J. Lendvai, T. Ungár, Investigation of Mg Loss during Heat-Treatments in an Al-Mg-Si Alloy, Mater Sci .Eng. 21 (1975) 169-175.

[4] J.P. Lynch, L.M. Brown, M.H. Jacobs, Microanalysis of age-hardening precipitates in aluminium alloys, Acta Metall. Mater. 30 (1982) 1389-1395.

[5] P. Dumitraschkewitz, P.J. Uggowitzer, S.S.A. Gerstl, J.F. Löffler, S. Pogatscher, Size-dependent diffusion controls natural aging in aluminium alloys, Nat. Commun. 10 (2019) 4746.

[6] P. Dumitraschkewitz, S.S.A. Gerstl, P.J. Uggowitzer, J.F. Löffler, S. Pogatscher, Atom probe tomography study of as-quenched Al-Mg-Si alloys, Adv. Eng. Mater. 19 (2017) 1600668.